

Cervical transforaminal ligaments on MRI and its clinical significance

Junlin Li

Inner Mongolia Autonomous Region People's Hospital

Lina Wang

Inner Mongolia Autonomous Region People's Hospital

Xiaoqin Zhang (✉ zxq1498@163.com)

Inner Mongolia Autonomous Region People's Hospital

Xuehui Ouyang

Inner Mongolia Autonomous Region People's Hospital

Research article

Keywords: Cervical vertebra, Transforaminal ligament, 3D-FIESTA, Cervical radiculopathy

Posted Date: July 24th, 2019

DOI: <https://doi.org/10.21203/rs.2.10743/v2>

License: © ⓘ This work is licensed under a Creative Commons Attribution 4.0 International License.

[Read Full License](#)

Abstract

Background This study examined cervical transforaminal ligament(TFL) displays in cadavers and living bodies using magnetic resonance imaging (MRI) and evaluated the correlation between nerve entrapment in the brachial plexus by the TFL and cervical radiculopathy(CR). **Methods** First, 6 normal intact adult cervical specimens were used to calculate the relevant capacity in displaying the cervical TFLs by the three-dimensional fast imaging employing steady-state acquisition (3D-FIESTA). Second, 10 patients with CR and 10 healthy subjects were selected to perform the 3D-FIESTA sequence scan at the C4-T1 intervertebral foramina. The TFL display rate was calculated, and its correlation with CR was analysed. **Results** The microscopic anatomical results showed that the cervical TFL incidence was 39.6%. The relative capacity of the 3D-FIESTA sequence in displaying cervical TFLs showed a 96.6% specificity and a 73.7% sensitivity. In the 10 patients with CR, cervical TFLs were present in 17 intervertebral foramina, of which, 10 cases showed hypertrophy of the TFLs causing nerve entrapment, and corresponding symptoms of CR were found in 8 cases of cervical TFLs. The correlation between nerve root entrapment by the cervical TFL and CR showed a 96.8% specificity and an 80% sensitivity. In the 10 healthy subjects, cervical TFLs were present in 13 intervertebral foramina. **Conclusions** The MR 3D-FIESTA sequence has high clinical value in displaying cervical TFLs in both cadavers and living bodies. If 3D-FIESTA sequencing shows nerve entrapment by the TFL, the possibility of CR caused by this TFL is approximately 80.0%. Conversely, the possibility of CR remains at 3.2%.

Background

Research on cervical TFLs is relatively rare. To date, few studies on cervical TFL anatomy have been reported [1–2], and imaging studies of the TFL are also rare. Many researchers believe that the presence of lumbar TFLs may cause lumbar and leg pain due to entrapped nerve roots [3, 4]. Shi et al.'s latest study [2] found that cervical TFL hypertrophy likely causes entrapment of the anterior branch of the corresponding cervical nerve, resulting in corresponding clinical symptoms and causing CR. Therefore, imaging studies of cervical TFLs should provide new approaches to diagnosing CR, as well as new surgical strategies for treating it, which have important clinical application value. In current research on the aetiology of CR, the TFL may be a new factor. The 3D-FIESTA sequence clearly displays the anatomic details because it has high soft tissue resolution, with increasing applications in clinical practice due to its short scanning time [5,6]. This study applied 3D-FIESTA sequencing to scan the intervertebral foramina of cervical spine specimens and confirmed its high clinical value in displaying the cervical TFL. The 3D-FIESTA sequence was then applied to a living cervical scan, and the results showed that TFL hypertrophy can cause nerve entrapment in the brachial plexus, demonstrating that TFL hypertrophy is correlated with CR.

Methods

1. Research objects

1.1. Cadavers:

Six adult intact cervical specimens (3 males and 3 females, aged 40–72 years, with an average age of 58 years) were provided by the Department of Human Anatomy, Southern Medical University and were selected for the study. Specimens with cervical trauma, deformity, or surgery were excluded.

1.2. Living study objects:

Patients with clinically diagnosed CR were selected. Cases were excluded if they had disc herniation or unobvious protrusion that was inconsistent with the clinical symptoms of resulting CR, cervical trauma or tumours, or hyperplasia and sclerosis of facet or Iuschka's joint that may lead to CR. Finally, 10 cases (5 males and 5 females, aged 41–65 years, with an average age of 54.7) were included. Ten healthy subjects were also selected (5 males and 5 females, aged 46–56 years, with an average age of 51.2). All met the inclusion criteria: no clinical symptoms of CR, no traumatic history, and no history of neck surgery.

2. Magnetic resonance examination

A 3.0T superconducting magnetic resonance scanner (Signa HDxt; GE Healthcare, Milwaukee, WI, USA), with a 16-channel head-neck combined phased-array coil was used to scan the specimens using a 3D-FIESTA sequence. The 3D-FIESTA sequence scan parameters were as follows: time to repetition (TR): 6.1 ms, time to echo (TE): 1.5 ms, flip angle: 60°, field of view (FOV): 14.0, matrix: 512×512, and slice thickness: 0.8 mm. The radiologists used the Advantage Workstation (AW 4.4 Workstation) system to observe the position, travel direction, and signal strength of the TFLs.

3. Evaluation

3.1. Evaluating the capacity of the 3D-FIESTA sequence to display the TFL using the anatomical observation results

A TFL dissected from a cervical corpse was used as a control standard to assess the 3D-FIESTA sequence's capacity to display the ligament. The calculation included the specificity, which meant the ability of the 3D-FIESTA sequence to determine when the specimen had no ligament, and the sensitivity, which meant the ability of the 3D-FIESTA sequence to identify when the ligament was present.

3.2. The level of nerve entrapment in the patients with clinically diagnosed CR was used as the standard, and the nerve entrapment of the intervertebral foramen at different levels was judged via the MR 3D-FIESTA sequence, thereby evaluating the correlation between the TFL and CR.

Clinically, the level of nerve entrapment is determined based on its symptoms. A 3D-FIESTA sequence scan was performed on this object to display the TFL and its relationship with the nerve root. The calculation included the specificity, or the 3D-FIESTA sequence's ability to show no ligament if no

entrapment was clinically determined on the nerve root, and sensitivity, or the 3D-FIESTA sequence's ability to display the ligament causing the nerve entrapment if nerve root entrapment was clinically determined. The calculation also included the positive predictive value, or the possibility that the 3D-FIESTA sequence would show the CR caused by the ligament entrapment when ligament entrapment was clinically determined, the negative predictive value, or the possibility that the 3D-FIESTA sequence would show no ligament entrapment when no ligament entrapment was clinically determined, and the accuracy, or the sequence's ability to determine that the CR was caused by ligament entrapment.

Results

1.1. 3D-FIESTA sequence scanning results for the cadaver specimens

The TFL signal differed from that of the nerve root, showing a low-signal linear structure (Fig.1-a). Fifteen TFL signals were observed in 48 MR imaging findings of intervertebral foramina. The number of TFLs found in each intervertebral foramen is shown in Table 1.

1.2. Anatomical study results for the cervical cadaver specimens

Among the 6 cervical cadaver specimens, 19 TFLs (Fig.1-b) were found in 48 C4-T1 intervertebral foramina (one of the intervertebral foramina had two TFLs). The TFL incidence varied greatly among the individuals. Some cervical specimens had multiple TFLs, while some specimens had none. The TFL incidences in the various C4-T1 segments are shown in Table 2.

1.3. Anatomical observations of the cervical specimens compared with the MR 3D-FIESTA sequence scanning results

The TFL results showed 14 true positives, 1 false positive, 5 false negatives, and 28 true negatives. The 3D-FIESTA sequence results for the cervical TFLs showed a 96.6% specificity and 73.7% sensitivity. Fig.1 shows an anatomical image of a TFL in a cervical specimen with its corresponding MR 3D-FIESTA sequence displaying the ligament.

2. Using the level of nerve entrapment from a case with clinically diagnosed CR as a reference, the MR 3D-FIESTA sequence was used to determine if any ligament entrapment occurred in different foraminal regions, and the correlation was then analysed.

The 3D-FIESTA sequence clearly showed the living cervical TFLs. The TFL signals were slightly lower than those of the brachial plexus (Fig.2).

Based on clinical manifestations of the 10 patients with CR, 13 TFLs causing nerve entrapment were identified. The 3D-FIESTA sequence revealed that 17 TFLs and 10 TFLs caused nerve entrapment, among which, the nerve entrapment caused by 8 TFLs matched the cases clinically diagnosed with CR. Based on clinical manifestations, the TFL should not be causing nerve entrapment in the healthy subjects. The 3D-FIESTA revealed 13 TFLs in the healthy subjects, with one causing nerve entrapment, but the subject had no clinical symptoms. 3D-FIESTA showed that the average display rate of the TFL in the patients with CR was approximately 21.3%, while the average display rate in the healthy subjects was approximately 16.3%. The display rates for the TFLs in all cervical C4-T1 spine segments are shown in Table 3.

The clinical data together with the 3D-FIESTA sequence scans resulted in 8 true positives, 2 false positives, 2 false negatives, and 61 true negatives. The healthy subjects' results included only 1 false positive and 79 true negatives. Fig.3 shows the MR 3D-FIESTA sequence of a living cervical TFL. The MR 3D-FIESTA sequence showed that the entrapment by the lateral TFL had a 96.8% specificity for the clinically diagnosed CR, with an 80% sensitivity. The positive predictive value was 80.0%, the negative predictive value was 96.8%, and the accuracy was 94.5%. The healthy subjects' specificity was 98.8%.

Discussion

Current research on TFLs focuses on the anatomy and mostly the lumbar vertebrae [7–9]. Studies on the cervical TFL are uncommon, with fewer imaging studies on TFLs. In this study, anatomic and imaging findings on TFLs in the cervical spine specimen were compared, and they confirmed that the MR 3D-FIESTA sequence clearly displayed the cervical TFLs. Furthermore, cervical spines from living bodies were examined, and for the first time, an imaging study was conducted of TFLs of living cervical spines.

Shi et al.'s [2] study showed that the incidence of cervical TFLs at the extraforaminal space of the intervertebral foramen is higher in the lower cervical vertebrae. The lower cervical spine is the location issuing the brachial plexus and is closely related to CR. Therefore, the intervertebral foramina from C4 to T1 were selected for this investigation. In this study, the average TFL display rate was approximately 35.0% on the cervical cadaver specimens and 22.8% on the living bodies. The TFL display rate in the imaging study with the living cervical spines was lower than that of the cadaver specimens, which may be related to the images' signal-to-noise ratio. Cervical cadaver specimen MR images contain no motion artefacts, while those of living cervical spines include unavoidable involuntary movements such as swallowing and blood vessel pulsation. This results in a reduced signal-to-noise ratio for the live image, which impacts the radiologists' analytical power in assessing the TFLs. However, we believe that with improved imaging equipment and technology, these motion artefacts can be reduced, and their impact can be minimized in future TFL analyses. In addition, cervical TFLs in different individuals differ greatly. Shi et al.'s study [2] showed that up to 7 cervical TFLs were found in some individuals, while no cervical TFLs were found in others. Therefore, the TFL display rates for the living bodies and cadaver specimens in our MR study may differ. At present, relatively few scholars are investigating cervical TFLs, with few cases in these studies. To more accurately understand the incidence of TFLs, the study's sample size must be increased, and multicentre research should be conducted in the future.

In clinically determining CR [10–11], Wainner et al. [11] found that more than 75% of patients were diagnosed with CR based on their clinical history. In this study, the nerve entrapment position was determined by the chief physician in neurology, who had been involved in clinically diagnosing cervical diseases for more than 20 years. When clinically diagnosing CR, subjective opinions may exist in individual cases, and objective and accurate indicators are lacking; thus, the results may be biased. Therefore, we conducted myoelectric evoked potential examinations in some patients [12] to further improve the accuracy in clinically diagnosing CR.

Our study showed that the correlation between nerve entrapment caused by the cervical TFL and CR had a 96.8% specificity, which is relatively high. This may be related to the absence of TFLs in most intervertebral foramina. The TFL display rate on the cervical spine in the 3D-FIESTA sequence was only 22.8%. Of the 22.8% TFL displays, only 58.8% showed entrapment, indicating entrapment in only 13.4% of the TFLs overall. Thus, only 13.4% of the TFLs in the foramina showed entrapment. In other words, when the nerve in the intervertebral foramen is clinically determined as not being entrapped, the radiologist can confirm that no TFL exists in this foramen, or the presence of a TFL did not cause nerve entrapment. The 80.0% sensitivity of the living cervical TFLs suggested a 20.0% possibility that the 3D-FIESTA sequence did not reveal the CR caused by nerve entrapment due to the TFL. This might suggest that the accuracy in clinically determining CR in this study was not 100%, and some cases were misdiagnosed. In the future, we will increase the number of examinations for clinically diagnosing CR by adding additional objective data, such as electromyography (EMG) examinations, to improve the clinical diagnostic capability, thereby better detecting the 3D-FIESTA sequence's display capacity in determining nerve entrapment caused by TFLs.

In the healthy subjects, the average display rate of the TFL by 3D-FIESTA sequencing was approximately 16.3%, while the average incidence of the TFL in the patients with CR was approximately 21.3%. This indicated a large difference in those with TFLs and indirectly reflected that the incidence of TFLs in patients with CR is higher than that in people without CR and the higher this incidence, the higher the probability of nerve entrapment. We conducted a comparative study of cervical spine specimens and MR 3D-FIESTA sequence scans to confirm that 3D-FIESTA sequencing clearly displays the cervical TFLs. 3D-FIESTA sequencing was applied to studying living cervical spines, confirming that nerve entrapment by the TFL is correlated with CR. Therefore, surgical treatment, such as releasing or removing the ligament, may be an option for treating CR in the future, which provides a good idea for clinical surgery. In the future, it may be possible to reselect the surgical plan.

Conclusion

MR 3D-FIESTA sequencing clearly displays the TFL and its relationship with the nerve root, both in cadaver cervical specimens and in living cervical vertebrae. If the 3D-FIESTA sequence shows that the nerve is compressed by a TFL, the possibility of CR caused by this TFL is approximately 80.0%. Conversely, the possibility of CR remains at 3.2%. MR 3D-FIESTA sequencing can confirm whether

entrapment of the nerve root by the TFL is causing the clinical symptoms of CR. It has a high clinical application value and provides a new idea and strategy for diagnosing and treating CR in the future.

Abbreviations

CR cervical radiculopathy MRI magnetic resonance imaging TFL transforaminal ligament

3D-FIESTA three-dimensional fast imaging employing steady-state acquisition

Notes And Declarations

Notes

Junlin Li and Lina Wang contributed equally to this work.

Declarations

Ethics approval and consent to participate

Current study was approved by the Inner Mongolia Autonomous Region People's Hospital and need for signed informed consent was waived.

Consent to publish

Not applicable

Availability of data and materials

The datasets used and/or analyzed during the current study available from the corresponding author on reasonable request.

Competing Interests

The authors have no conflicts of interest relevant to this work.

Funding

This study was supported by the Natural Science Foundation of Inner Mongolia No. 2017MS(LH)0850; In the role of collection data.

Authors' contributions

JLL and LNW participated in the design of the study and drafted the manuscript, XHOY collected the patients' data, and processed the figures. XQZ conceived the study and supervised the project. All authors read and approved the final version of the manuscript.

Acknowledgements

Not applicable

References

- [1] Arslan M, Açar Hİ, Cömert A. Cervical extraforaminal ligaments: an anatomical study[J]. *Surg Radiol Anat.*2017; 39(12):1377–83.
- [2] Benchao Shi, Xuefeng Zheng, et al. The Morphology and Clinical Significance of the Extraforaminal Ligaments at the Cervical Level[J]. *Spine (Phila Pa 1976).*2015; 40(1):E9–17.
- [3] Min JH, Kang SH, Lee JB, et al. Anatomic analysis of the transforaminal ligament in the lumbar intervertebral foramen[J]. *Neurosurgery.*2005; 57(1 Suppl): 37–41; discussion 37–41.
- [4] Marić DL, Krstonošić B, Erić M, et al. An anatomical study of the lumbar external foraminal ligaments: appearance at MR imaging[J]. *Surg Radiol Anat.*2015; 37(1): 87–91.
- [5] Amemiya S, Aoki S, Ohtomo K. Cranial nerve assessment in cavernous sinus tumors with contrast-enhanced 3D fast imaging employing steady-state acquisition MR imaging[J]. *Neuroradiology.*2009; 51(7): 467–70.
- [6] Nemoto O, Fujikawa A, Tachibana A. Three-dimensional fast imaging employing steady-state acquisition MRI and its diagnostic value for lumbar foraminal stenosis[J]. *Eur J Orthop Surg Traumatol.* 2014; 24 Suppl 1:S209–14.
- [7] Zhao Q, Zhong E, Shi B, et al. The morphology and clinical significance of the intraforaminal ligaments at the L5-S1 levels[J]. *Spine J.*2016;16(8):1001–6.
- [8] Akdemir G. Thoracic and lumbar intraforaminal ligaments[J]. *J Neurosurg Spine.*2010;13(3):351–5.
- [9] Zhong E, Zhao Q, Shi B, et al. The Morphology and Possible Clinical Significance of the Intraforaminal Ligaments in the Entrance Zones of the L1-L5 Levels[J]. *Pain Physician.*2018; 21(2):E157-E165.
- [10] Childress MA, Becker BA. Nonoperative Management of Cervical Radiculopathy[J]. *Am Fam Physician.*2016; 93(9):746–54. Review.

[11] Wainner RS, Gill H. Diagnosis and nonoperative management of cervical radiculopathy[J]. J Orthop Sports Phys Ther.2000; 30(12): 728–44.

[12] Troni W, Benech CA, Perez R, et al. Non-invasive high voltage electrical stimulation as a monitoring tool of nerve root function in lumbosacral surgery[J]. Clin Neurophysiol.2013; 124(4):809–18.

Tables

Table 1. Number of TFLs in each segment of the cadavers in the MR imaging

Intervertebral foramen	TFL (left)	TFL (right)
C4-C5	1	1
C5-C6	1	3
C6-C7	3	2
C7-T1	3	1
Total	8	7

Table 2. Anatomical indications of the number and incidence of TFLs in the C4-T1 intervertebral foramina

Intervertebral foramen	Number of intervertebral foramina showing the TFL	Incidence
C4/C5	3	25%
C5/C6	5	42%
C6/C7	5	42%
C7/T1	5	42%

Table 3. Number and display rates of the C4-T1 TFL segments by MR 3D-FIESTA sequencing

Intervertebral foramen	Number of intervertebral foramina showing the TFL	display rate
C4/C5	7	18%
C5/C6	7	18%
C6/C7	10	40%
C7/T1	6	15%

Figures

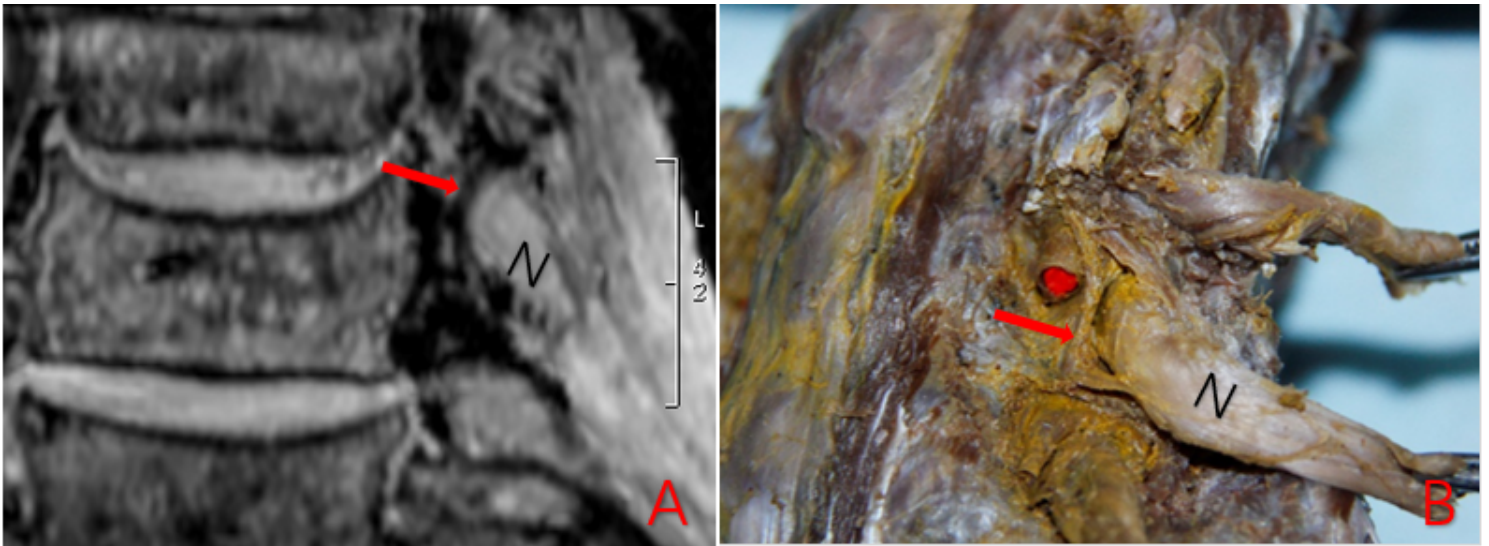


Figure 1

a Coronal image after 3D reconstruction of 3D-FIESTA sequence of cervical specimen. The red arrows in the T2W images indicate the TFL shown in the anatomical image of the same cadaver specimen. The TFL presented low-intensity signals. b Anatomical image of the TFL (indicated by a red arrow) on the left side of the IVF between C6 and C7 of cervical specimen. N stands for Nerve root.

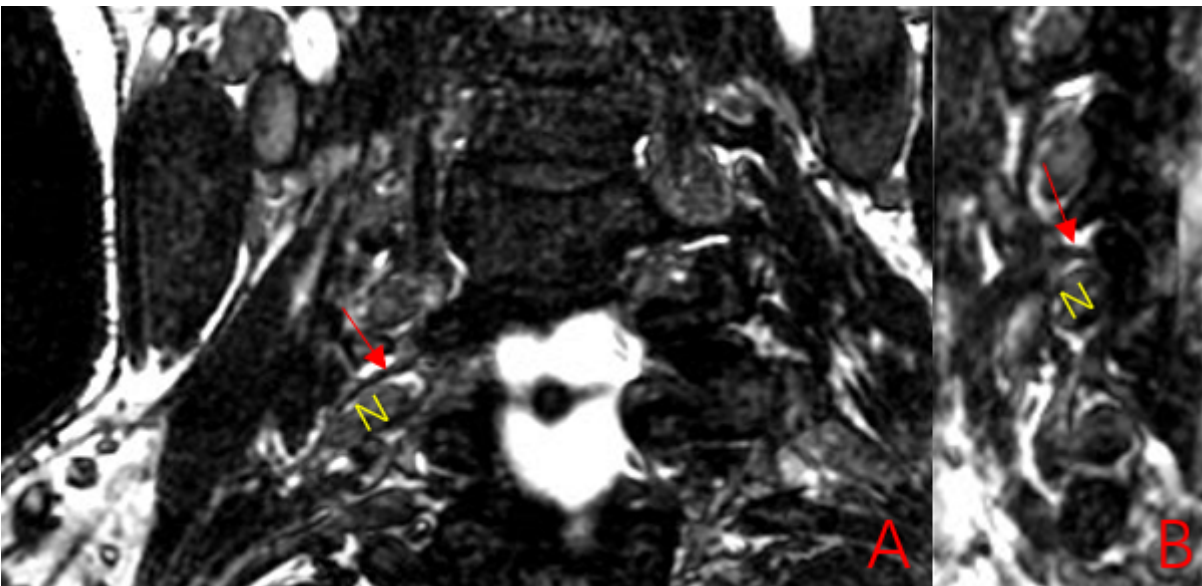


Figure 2

3D-FIESTA sequencing shows the TFL in the C6-7 intervertebral foramen of the right living cervical spine: a oblique coronal position; b oblique sagittal position, showing the linear TFL (arrow) in a low signal above the extraforaminal nerve root (N), with the nerve root (N) showing a slightly higher signal. The TFL starts at the lower edge of the upper transverse process and ends at the upper edge of the lower transverse process.

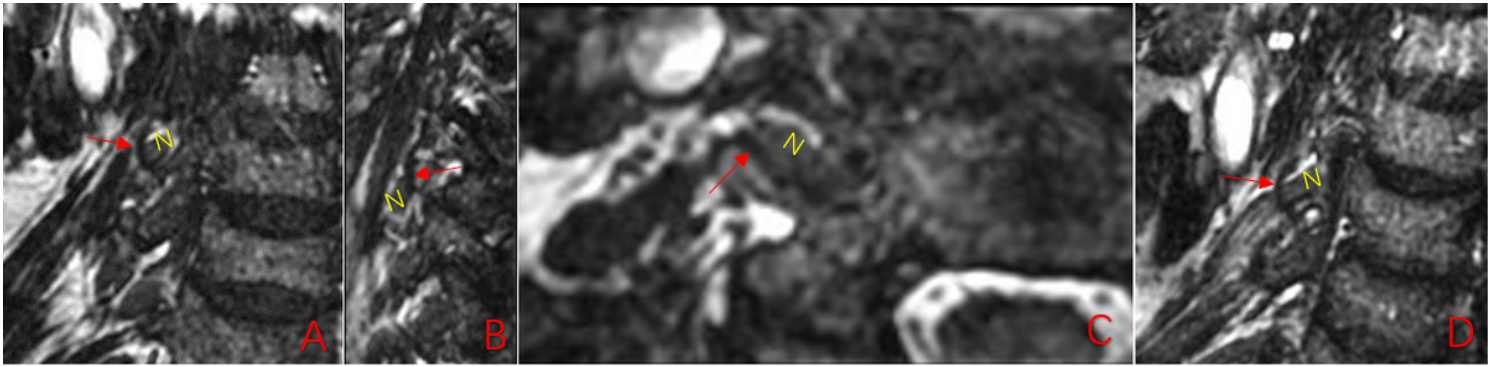


Figure 3

3D-FIESTA sequencing shows the TFL in the C4-5 intervertebral foramen of the right living cervical spine. The linear TFL (arrow) in the low signal is in front of the extraforaminal nerve root (N), with the nerve root (N) in a slightly higher signal. The TFL starts at the lower edge of the upper transverse process and ends at the upper edge of the lower transverse process. The TFL is above the rear of the nerve root and presses against the nerve root, causing distortion of the nerve root (d). a, d are the oblique coronal position, b is the oblique sagittal position, and c is for the horizontal axis position.